Article

Fault Detection and Isolation of Load Mutation Caused by Electrical Interference of Single-Shaft Combined Cycle Power Plant

Kun Yao [1,2], **Ying Wang** [3], **Zongjie Li** [4], **Jiajia Li** [4], **Jie Wan** [2,4,*] **and Yong Cao** [1]

1   School of Mechanical Engineering and Automation, Harbin Institute of Technology (Shenzhen), Shenzhen 518055, China
2   Laboratory for Space Environment and Physical Sciences, Harbin Institute of Technology, Harbin 150001, China
3   College of Power and Energy Engineering, Harbin Engineering University, Harbin 150009, China
4   School of Energy Science & Engineering, Harbin Institute of Technology, Harbin 150001, China
*   Correspondence: wanjie@hit.edu.cn

Abstract: Because the generator power-measuring equipment is often accompanied by electrical interference in a complex electromagnetic environment in an actual thermal power plant, the output signal will change or even distort while it passes through the devices of acquisition and conversion. Several practical cases have found that the abnormal generation change phenomenon, impulse or oscillation caused by electrical interference, has different effects on the load regulation of steam turbines. These faults also exist in combined-cycle power plants (CCPPs). However, the insufficient installed capacity and operating life of CCPPs domestically cause similar load mutation failures that are scarcely found. We had to acknowledge that CCPPs and steam turbine regulation characteristics differ. It is of great value to study the influence of differences in load mutation on the load regulation of single-shaft CCPPs. We extracted the fault characteristics of two sudden load change phenomena using the operation data of an actual steam turbine and analyzed them through simulation. Furthermore, a fault detection and isolation method for sudden load changes in a single-shaft CCPP was proposed and the simulation results verified the method's effectiveness.

Keywords: combined-cycle power plant; steam turbine; load mutation; fault detection and isolation; electrical interference

1. Introduction

The random fluctuation characteristics of renewable energy sources lead to sudden load changes in their power generation processing [1]. This load mutation problem affects the generator's regulation and the power grid's stability [2]. Therefore, a stable and reliable power supply is required to smooth the defects in renewable energy sources [3]. The gas turbine in a CCPP has a wide and flexible regulating ability of generation, making it increasingly important to achieve a stable frequency and peaking regulation of the power grid, especially for the potential threats to grid-connected stability of renewable energy [4,5]. Similarly, it also leads to an increasing number of CCPPs taking on more of these tasks [6]. Numerous factors can lead to the phenomenon of load mutation in CCPPs, some of which are beneficial and some of which are harmful. For example, using the characteristics of rapid and flexible regulation of the CCPP to smooth the sudden load changes caused by renewable energy helps maintain the grid's stability. The consistency between load and generation is an important indicator for evaluating the generation performance of CCPPs. The sudden load changes can affect not only the regulation of the unit, but also the grid's stability [7]. Therefore, studies have focused on predicting the power output of CCPP [8,9]. Lorencin et al. [10] developed a GA-based multilayer perceptron (MLP) model with four parameters as inputs for the power output prediction of CCPPs. This idea is also applied to five machine learning (ML) algorithms and provides better prediction performance

with a gradient-boosted regression tree (GBRT) [11]. However, such methods are mostly applied to CCPP operating under full-load conditions rather than CCPPs with peaking and frequency regulation tasks. This means that methods are unsuitable for the CCPP with the tasks of peak load and primary frequency regulations and cannot predict the load-mutation fault of the CCPP effectively. More tasks of peak load and primary frequency regulations and more load-mutation faults in the CCPP could occur under means working under off-design conditions. In particular, for a CCPP with a single-shaft arrangement, the sudden failure of some components can easily trigger sudden changes in the power output. These load-mutation faults will affect the power grid's stability and reduce the unit's service life.

Fault diagnosis or early warning strategies using different algorithms were used during the monitoring process [12], that is, diagnosis of leaks in different equipment of the heat recovery steam generator (HRSG) [13] and fault tolerance for gas turbine measurement systems [14]. Camporeale et al. [15] analyzed the impact of various equipment faults on the measurements and performance of CCPP. They proposed a fault diagnosis method with a two-layer feed-forward neural network to classify 11 faults in gas turbines, HRSG, and CCPP generators. Finn et al. [16] discussed different assessment methods for the operational status of the CCPP and a lot of operational data verified the validity of these methods.

Although the above diagnostic algorithms have achieved good accuracy in various datasets, considerable noise and diversity of fault categories in the actual environment always weaken their effectiveness [17]. There is also a fault summarized as an electrical interference fault on the generator that will lead to load mutation failure of the CCPP in addition to these common equipment failures. More specifically, there is a large deviation between the actual power value and the measured value of the power output caused by excessive interference from the working environment, aging of components, or disturbance of the power grid. Unlike a common sensor fault, this fault is not an abnormal power signal caused by the fault of the sensor itself but the electrical interference on the generator that then acts on the signal measurement system, resulting in an abnormal disturbance in the power measurement signal [18]. This fault not only causes adverse effects on the grid stability but also increases the adjustment frequency and shortens the component service life of the CCPP. Therefore, it is significant to study the influence of different load-mutation faults caused by electrical interference on the single-shaft CCPP and to establish an isolation method for load mutation of the CCPP.

By extracting the characteristics of load-mutation faults caused by electrical interference on a turbo generator set, the impact of such faults on the CCPP was analyzed in a simulation model of a single-shaft CCPP. The remainder of this paper is organized as follows. Section 2 provides a mechanical analysis of the two load-mutation faults caused by electrical interference. Section 3 describes the modeling of the single-shaft CCPP and Section 4 presents a simulation analysis and a discussion of the two faults. Finally, a diagnostic isolation method for sudden load change faults in CCPP is proposed and simulated based on the above research in Section 5.

2. Fault Analysis of Load Mutation Caused by Electrical Interference

The generator set's automatic gain control (AGC) is the basis for the unit to achieve a stable power output or variable load capability. The control performance of the generator set deteriorates and is very likely to cause sudden load change failure when working in a disturbed environment, aging equipment, or grid disturbances. Generation, the key indicator of a unit's generating capacity, can affect its life and economy when a load-mutation fault occurs. Load mutations caused by electrical interference can be categorized into pulses and oscillations [18]. This fault is related only to the generator and electrical system rather than its thermal system. Despite the lack of such failure data for single-shaft CCPPs, many domestic coal-fired units with long operating lives could provide a lot of historical data to extract fault features of load mutation. We can draw on the fault data

of the electrical interference of coal-fired units with the same capacity to analyze the fault characteristics of such faults in detail.

2.1. Pulsing Load-Mutation Fault

Pulsing load mutation is a fault with a sudden load change (increase or decrease) and returns to normal values within a short period [18]. Figure 1 shows the actual load historical data of a 300 MW coal-fired unit. Pulsing load mutations frequently occur in units owing to electrical interference. This abnormal state causes the unit to change flow demand energy management (FDEM), a comprehensive steam flow demand for steam turbines, to ensure that the actual load output matches its AGC command.
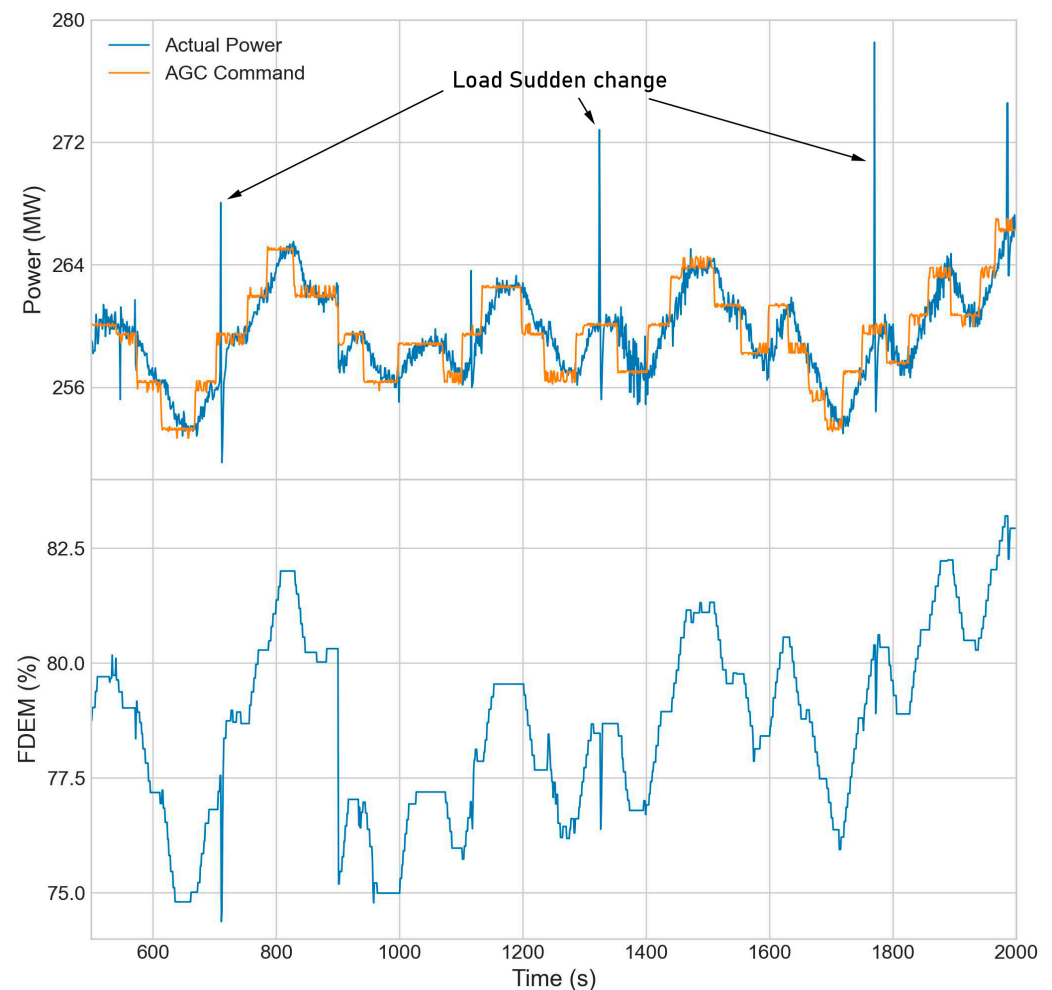

Figure 1. Pulsing load mutation.

The characteristics of pulsing load mutation can be obtained by comparing many sudden load change faults. As shown in Figure 1, the period of the pulsing load fault is maintained at 1~2 s and the magnitude of the fault is variable; that is, the fault magnitude at 1770 s is approximately 19 MW. Because of the slow regulation rate of the coal-fired unit, its regulation command is still not transmitted to the actual load after the pulsing load fault returns to a normal value. Therefore, the pulsing fault data for the actual load during normal operation can be considered as data for the sudden change in this load during the open-loop regulation of coal-fired unit.

The above analysis makes it possible to extract a specific sudden load change fault characteristic. When a pulsing load mutation occurs, the load corresponds to a pulse signal with a pulse width of 2 s and a pulse amplitude of 6.3% Pe (rated load), superimposed on the stable output of the unit's thermal system. The fault characteristics of the pulsing

load mutation of a coal-fired unit with the same capacity are mapped onto the open-loop regulation process of single-shaft CCPPs as the fault characteristics of the pulsing fault of a single-shaft CCPP.

2.2. Oscillating Load-Mutation Fault

Not all the load mutations caused by electrical interference are of the pulsing type described in the previous section, but there is also an oscillating load-mutation fault. The timing diagrams for the AGC command, actual generated load, FDEM, and pressure of the governing stage are shown in Figure 2. The peak-to-peak value of the load is only 0.4 MW. Nevertheless, load fluctuations occurred at 1680–2000 s and the value expanded to 1.8 MW within 20 s. Compared with the actual load variation trend, the reverse action and hysteresis of the FDEM indicate the stability of the thermal system. However, frequent fluctuations in the excitation current indicate that this load oscillation was caused by electrical interference, with fluctuations peaking at approximately 10 A.
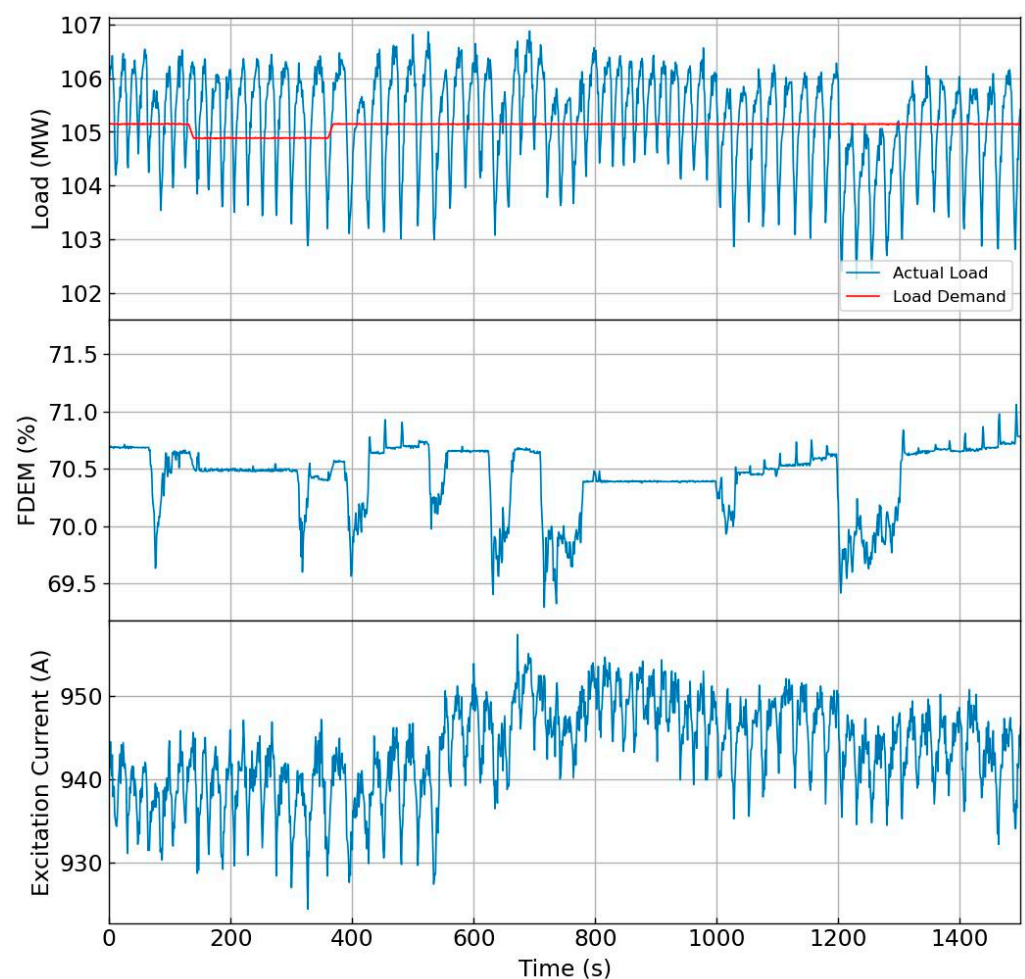

Figure 2. Oscillating load mutation.

The above analysis allows us to extract a specific fault characteristic of load oscillation caused by electrical interference. When a fault with frequent load oscillation occurs, the unit load corresponds to a sine wave signal with 20 s and an amplitude of 0.6% Pe superimposed on the stable output of the unit's thermal system.

3. Mathematical Modeling of CCPP

3.1. CCPP Modeling

A CCPP is a power unit that combines a steam turbine cycle with a gas turbine cycle. As shown in Figure 3, the exhaust of the gas turbine was fed into the HRSG to heat the steam and drive the steam turbine. Here, the CCPP modeling was selected as a unit with a single-shaft arrangement. This is a special arrangement in which the gas turbine, generator, and turbine are arranged on the same shaft. In this case, the gas turbine and steam turbine simultaneously provide power to one generator. In the modeling process, the modules for the gas turbine, HRSG, and steam turbine were built separately using a modular modeling approach and finally combined to form a dynamic simulation model of the CCPP [19].

Figure 3. Schematic of the single-shaft CCPP. HP—high-pressure turbine, IP—intemediate-pressure turbine, LP—low-pressure turbine, SH—superheater, RH—reheater, EV—evaporator, FP—feed water pump, RP—recycle pump, CP—condensate pump.

3.1.1. Gas Turbine

A gas turbine consists mainly of a compressor, combustion, and turbine. The same modular modeling approach was used to create modules for each component separately. In this case, the compressor and turbine were modeled using a table look-up approach and the equations required in the modeling process are shown below [20,21].

$$\left(\frac{g\sqrt{T_{in}}}{p_{in}}, \eta \right) = f\left(\pi, n/\sqrt{T_{in}} \right), \tag{1}$$

$$T_{out} = T_{in}\left(1 + \frac{1}{\eta}(\pi^{(k-1)/k} - 1) \right) \tag{2}$$

$$P_c = g c_p (T_{out} - T_{in}) \tag{3}$$

$$\frac{dP_3}{dt} = \frac{R_g T_g}{V}(g_{in} + g_b - g_{out}) \tag{4}$$

$$\frac{dT_3}{dt} = \frac{[g_{in}h_{in} + g_b(h_b + \eta_b LHV) - g_{out}h_{out}]}{\tau_{cc}g_{out}c_{pout}} \tag{5}$$

$$\frac{dn}{dt} = \left[\frac{30}{\pi} \right]^2 \frac{1}{J_1 N}\left(P_t - P_c - P_f - P_E \right) \tag{6}$$

where g is air flow; T is temperature; n is rotational speed; k is specific heat ratio; π is pressure ratio of per sub-module; η is efficiency; LHV is low calorific value of fuel; h is enthalpy; t is time; P is power output; c_p is constant-pressure specific heat capacity; τ_{cc} is time constants; ω is angular velocity; J is rotational inertia; P_E is load power; P_f is the power consumed owing to mechanical losses, drive assist systems, etc. The subscript of each parameter can be summarized as follows: *in* is the inlet parameter of the component, *out* is the outlet parameter of the component, *c* is the compressor, *t* is the turbine, and *b* means combustion.

3.1.2. HRSG Modelling

The HRSG in Figure 3 is a triple-pressure reheat waste-heat boiler. The mathematical model of the HRSG includes several modules, such as the heat exchange calculation of the water wall, evaporating heating surface, and superheater. Each module's energy exchange was calculated using the following equation:

$$Q_r = \alpha A \left(\frac{T_{in} + T_{out}}{2} - T_P \right), \tag{7}$$

$$T_{out} = T_{in} - \frac{Q_r}{c_Y g_Y} \tag{8}$$

$$S_G = \frac{1}{T_2 S + 1} Q_r \tag{9}$$

$$S_G - S_F = C_B \frac{dP_d}{dt} \tag{10}$$

$$P_d - P_T = K_{sh} S_F^2 \tag{11}$$

where Q_r is heat exchange; α is convection heat transfer coefficient; A is effective heat exchange area; T_{in} is gas turbine exhaust temperature; T_{out} is exhaust temperature of HRSG; T_P is saturation temperature at saturation pressure of the steam; c_Y is the specific heat capacity of the flue gas; g_Y is the flow rate of flue gas; S_G is the total effective heat absorption of the HRSG-heated surface; T_2 is the time constant of the heat transfer process of HRSG; P_d is the boiler drum pressure; S_F is the flow rate of superheated steam; C_B is the heat-storage coefficient of the boiler drum; P_T is main steam pressure; K_{sh} is the resistance coefficient of superheater pipeline.

3.1.3. Steam Turbine Modelling

The power output of the steam turbine is regulated by the sliding pressure operation, the high-pressure valves of which are fully open. This control mode can effectively utilize the energy in the gas turbine exhaust, thereby improving the energy utilization efficiency of the unit. The steam turbine can be described using the Flügel formula. The detailed calculation process can be found in Ref. [22]. In addition, we introduced the nozzle volume model and reheat volume model, as shown in Figures 4 and 5.
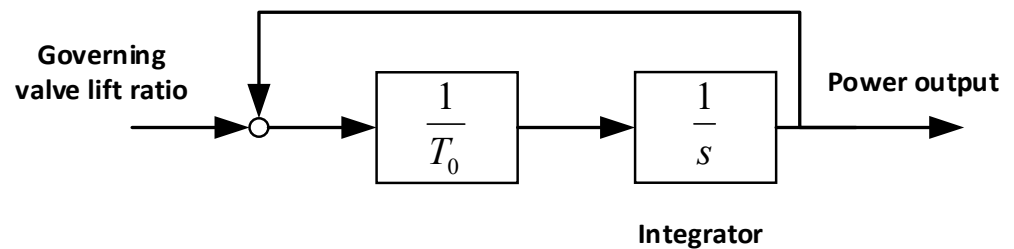

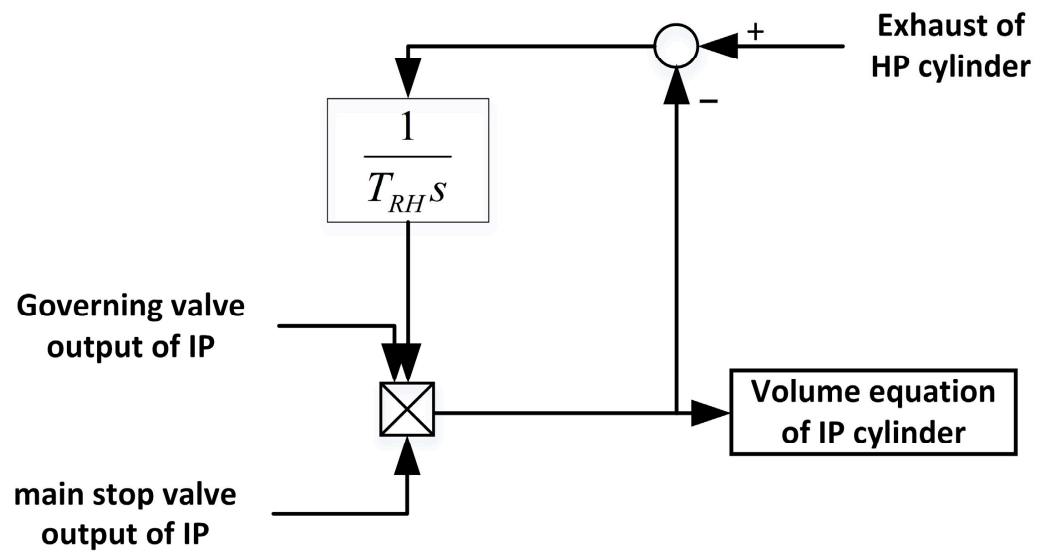**Figure 4.** Nozzle Volume Model.

Figure 5. Reheat system model.

3.2. Fault Setting

The fault characteristics, that is, the amplitude and period of the oscillating load mutation and the amplitude and duration of the pulsing load mutation, can be extracted from the fault analysis in Section 2. As shown in Figure 6, the fault characteristics obtained from Section 2 can be used as the fault data of the single-shaft CCPP with open-loop regulation. The data with these faults of the CCPP can be obtained through the dynamic model of the single-shaft CCPP established in Section 3. More specifically, the fault characteristics extracted in Section 2 are superimposed on the power output of the thermal system, which is regarded as the input entering the load controller and participating in the closed-loop control of the CCPP model. All parameters used in this section except time are per unit value (p.u.).
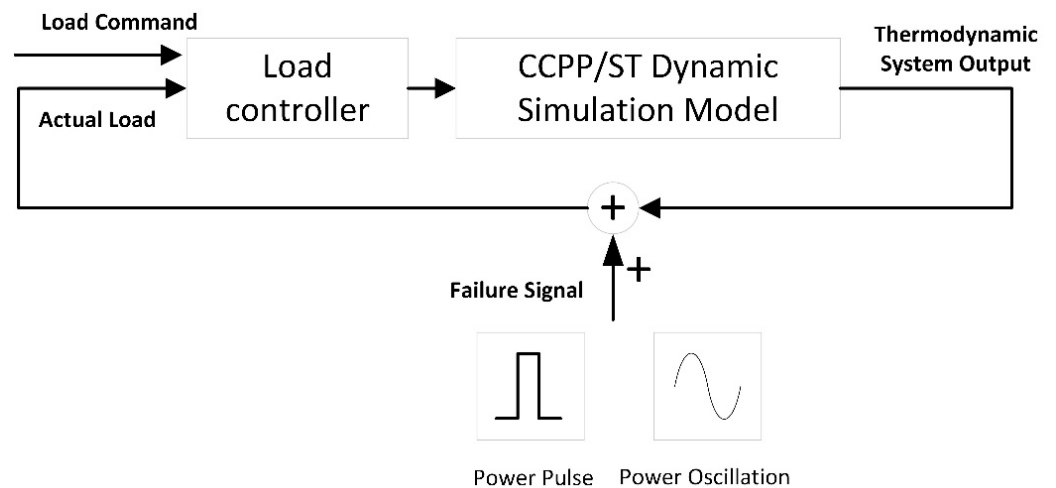
Figure 6. Fault simulation model of single-shaft CCPP.

4. Results and Discussion of Load Mutation

4.1. Simulation and Analysis of Pulsing Load Mutation

As shown in Figure 7, a pulse with a pulse width of 2 s and amplitude of 6.3% Pe is superimposed on the power output of the CCPP model, which is regarded as the input entering the load controller and participates in the closed-loop control of the CCPP model. Figure 7 shows the curves of the single-shaft CCPP and steam turbine (ST) during the normal state and the pulsing load mutation was obtained by simulation. The load command generates a large deviation from the actual load of the unit when there is a pulse in power

output. The CCPP and ST were adjusted to the amount of fuel in the combustor or steam flow in the ST to smooth the deviation. The CCPP regulates more quickly and corrects the power output simultaneously. However, the deviation between the actual power output and the load command of the CCPP is larger than that of the ST when the pulse signal recovers to the normal state, which increases the regulation of the CCPP. Because regulating the frequency of some components, that is, the fuel control valve, directly affects its chronological age, the pulsing load mutation caused by electrical interference can ultimately damage the service life of the critical equipment of the CCPP [23].
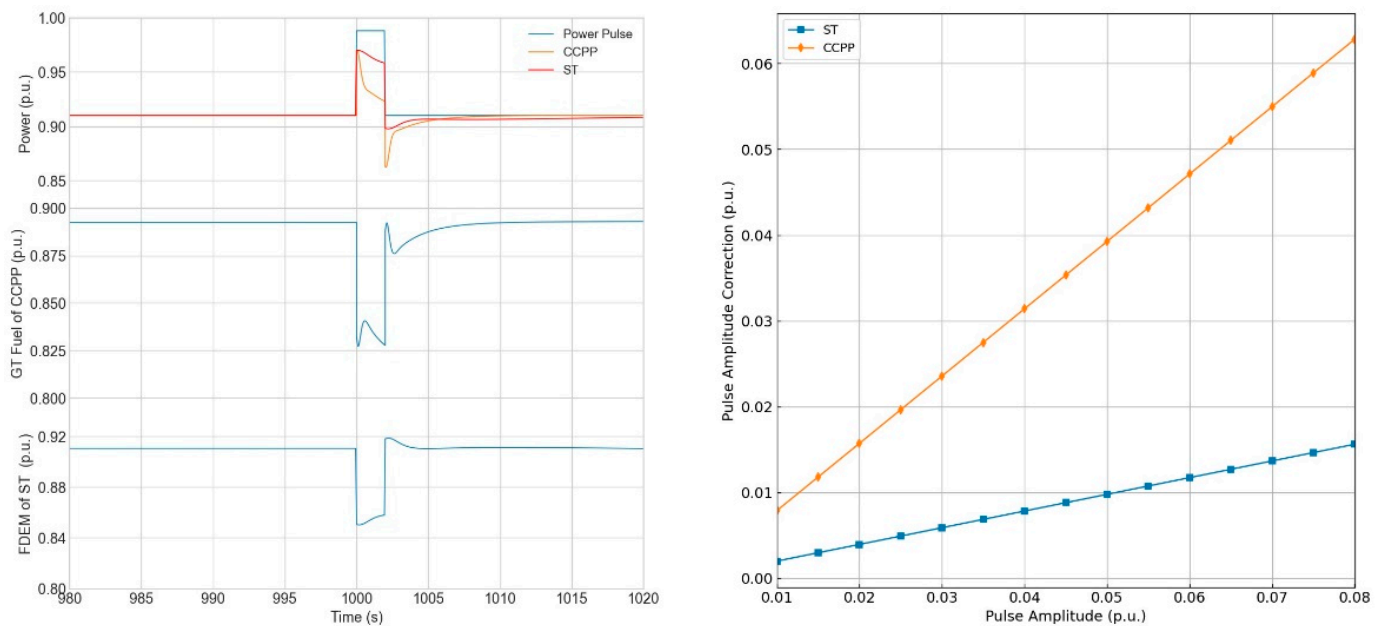
Figure 7. Pulsing load mutation of CCPP and ST.

Further study was conducted on how the pulse amplitude influences the load correction of the CCPP and ST, as shown in Figure 7. The load correction increased with the pulse amplitude. Compared to ST, CCPP has a larger load correction for the same pulse amplitude condition.

4.2. Simulation and Analysis of Oscillating Load Mutation

4.2.1. Simulation and Analysis of Oscillating Load Mutation

As shown in Figure 8, an oscillating signal, a sine wave signal with 20 s, and an amplitude of 0.6% Pe is superimposed on the power output of CCPP's thermal system as the actual measured unit load. The amplitude of load oscillations in the CCPP is reduced to 0.2% Pe. However, the fluctuation amplitude of the steam turbine is close to 0.6%. The pulse amplitude is defined above, indicating that the regulating characteristics of the CCPP are better than those of the steam turbine. The fast regulation characteristic of the CCPP makes it more effective in smoothing out the actual load changes that contain the oscillation signal. Figure 8b shows the change curves of the disturbance signal, actual load, gas turbine power, and steam turbine power in the CCPP. The asynchronous properties of the gas turbine and steam turbine in the CCPP during the load regulation process, that is, the phase of the actual power output of the gas turbine and steam turbine, are inconsistent.
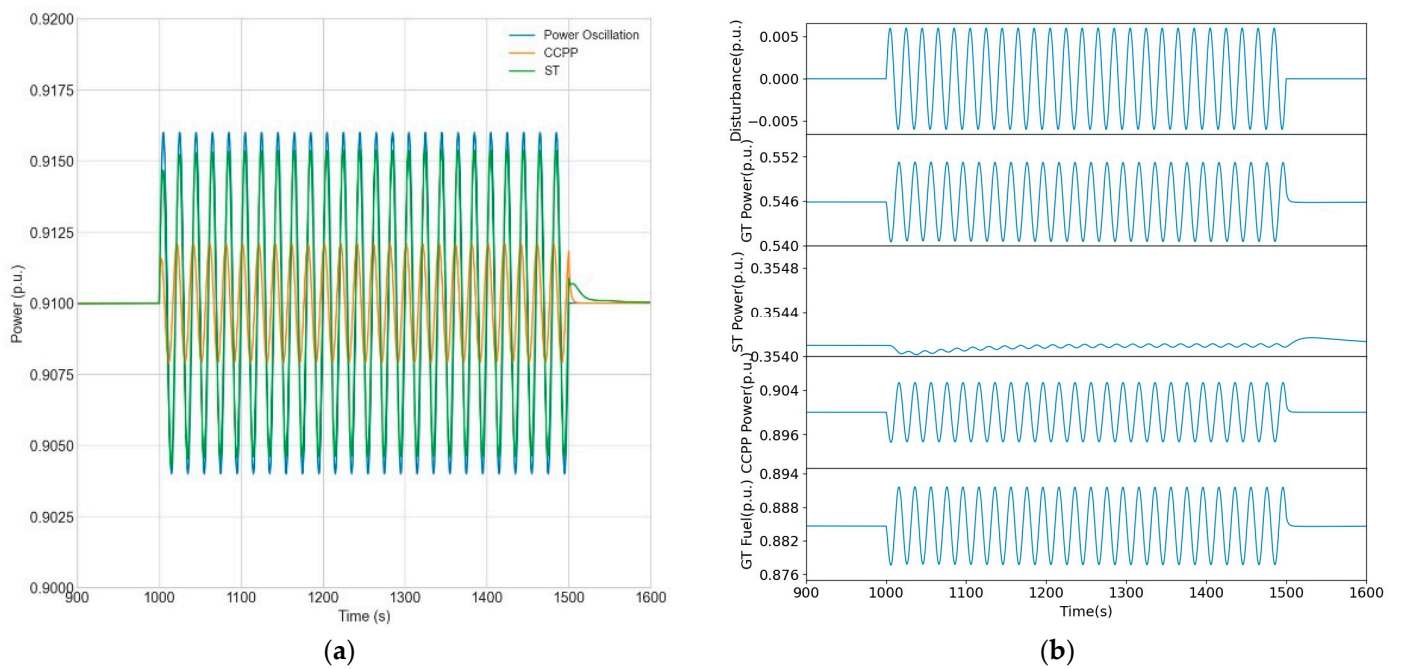
(**a**)

(**b**)

Figure 8. Simulation of oscillating load mutation. (**a**) Oscillating load mutation for CCPP and ST. (**b**) Load variation for CCPP.

4.2.2. Effect of Load Oscillation Period on the Simulation Results of Two Simulation Models

The effect of the oscillating load-mutation fault on the CCPP model was simulated with oscillating periods ranging from 2 to 60 s (2 s intervals), with 30 operating conditions, including three load states, 4% Pe, 6% Pe, and 8% Pe, as shown in Figure 9. The oscillating period of the actual load of CCPP decreases continuously as the oscillation period increases.

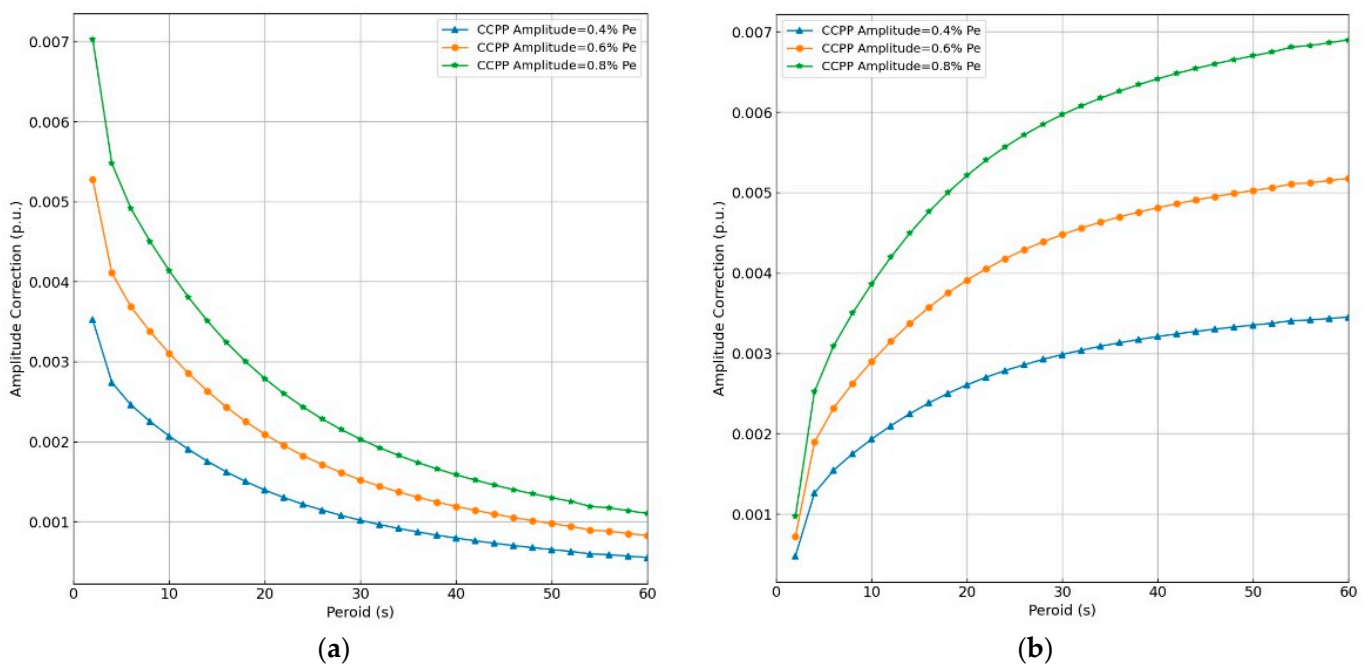(**a**)

(**b**)

Figure 9. Oscillating load-mutation faults of CCPP. (**a**) Amplitude Value. (**b**) Amplitude Correction Value.

5. Analysis of Fault Isolation Methods for Pulsing Load Mutation

5.1. Fault Isolation Scheme for Pulsing Load Mutation

From the above analysis, a pulsing fault produces a large load deviation, which causes a larger regulation of the CCPP, exacerbates the wear and tear of its component, and seriously affects its service life. Therefore, it is important to reduce the regulating frequency of the CCPP to extend its service life when a pulsing fault occurs.

The load signal cannot represent the power output of the unit when a pulsing fault occurs. Therefore, the load was not a feedback signal for the load control system. Otherwise, the electrical interference fault is transmitted through the load control system, which affects the regulation of fuel quantity. Because pulsing faults caused by electrical interference are characterized by rapid changes and recovery to a normal state, a variable load quantity is used to determine whether a pulsing fault has occurred. A pulsing fault is considered to have occurred when the load variable quantity per second exceeds 0.5% Pe.

Considering that the pulse width of a pulsing fault generally does not exceed 2 s, a fault isolation scheme for an electrical interference fault in a single-shaft CCPP is proposed, as shown in Figure 10. After detecting a pulsing load mutation, a pulse with a pulse width of 2 s was triggered. The load command temporarily replaced the unit load as a feedback signal to the unit load during these 2 s. After the pulse signal disappears and the unit load recovers to a normal value, the unit load is reintroduced as a feedback signal directly into the unit load control system to ensure normal regulation of the unit. In other words, we establish a one-out-of-two system using the two values of the load command and actual load. When load mutation occurs, the actual load is temporarily chosen as the feedback signal to the load control system during the regulation process. When this fault was eliminated, load commands were used in the control system during the regulation process.
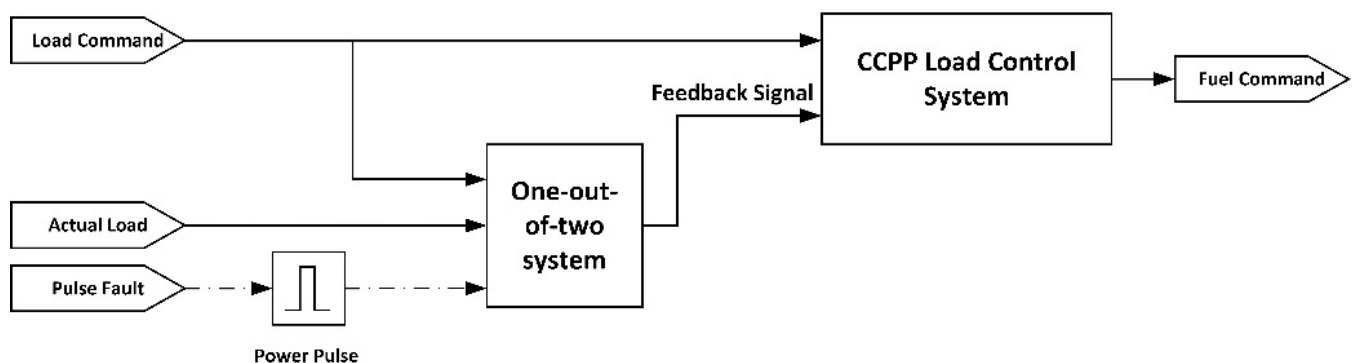

Figure 10. Fault isolation scheme for pulsing faults in single-shaft CCPP.

5.2. Results and Discussion of Fault Isolation Method

Figure 11 shows the simulation results for the model with different control methods. The control method without fault isolation is shown in Figure 11a. The power output of the CCPP changes following the pulsing load mutation under this control method, which results in a large load disturbance because the fuel consumption of the gas turbine follows the regulation. However, by comparing with the control method in Figure 11b, the load disturbance of the CCPP caused by electrical interference can be effectively suppressed. Figure 11 shows that the power output of the CCPP with the fault isolation algorithm changes stably when it is controlled by the AGC command. Regardless of whether the electrical interference has a positive value, the fault isolation method can effectively eliminate the influence of this interference on the regulation of CCPP.
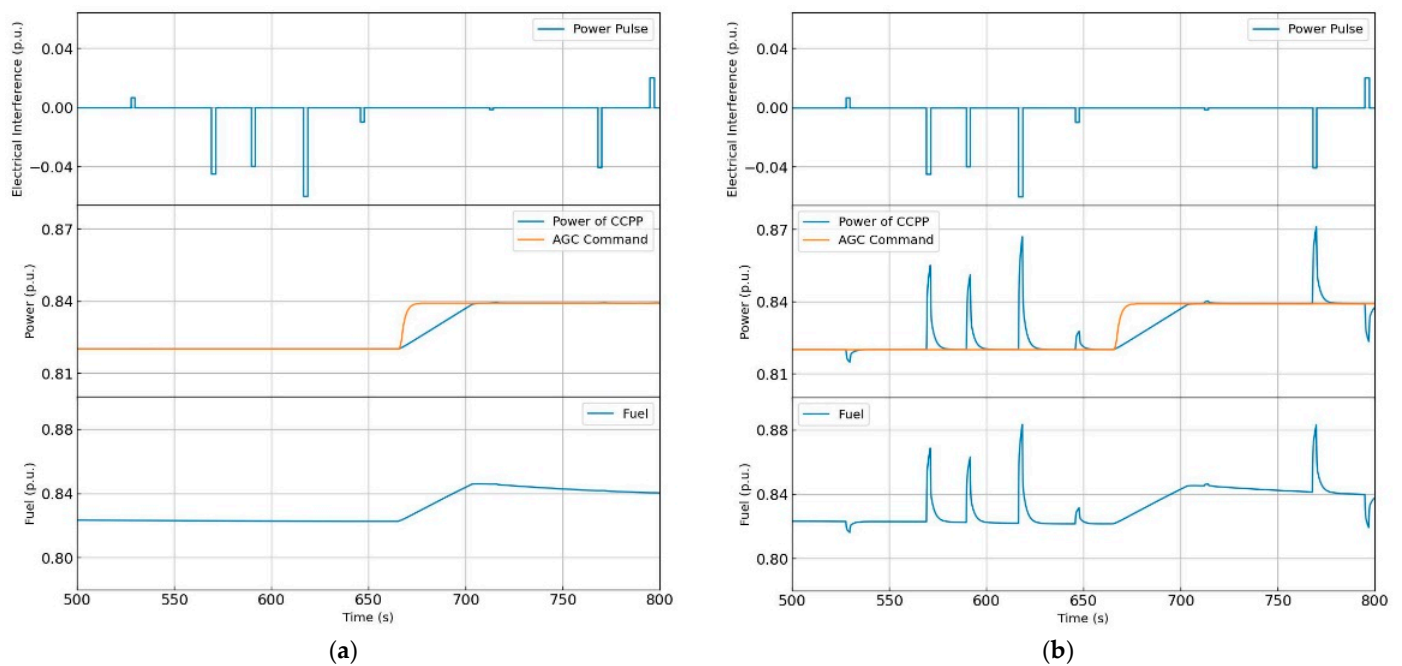
Figure 11. Simulation with different control methods. (**a**) Simulation with fault diagnosis isolation method. (**b**) Simulation without fault diagnosis isolation method.

6. Conclusions

The complex electromagnetic environment affects the device performance of the electrical system in the generator, such as set-signal acquisition and conversion, which generates signal interference in the signal system. This study analyzed load-mutation faults in generator sets caused by signal interference in an electrical system. By extracting the fault characteristics based on the load-mutation fault data in the ST set, a CCPP model was built to analyze the impact of load mutation on the CCPP. Finally, a corresponding fault diagnosis and isolation method was proposed to ensure the safe and smooth regulation of the CCPP.

Drawing on electrical fault data from coal-fired units, the fault characteristics of the load mutation during the open-loop regulation of a single-shaft CCPP were refined. Compared with oscillating load mutation, pulsing load mutation has a more serious impact on the load regulation of CCPP. It is also a type of fault that needs to be isolated.

A fault isolation scheme for a single-shaft CCPP was proposed. For pulsing load mutation, replacing the load command with the power output of the CCPP temporarily as a feedback signal to its load control system when a pulsing load mutation occurs can ensure the fuel quantity command and unit operation stability.

Author Contributions: Conceptualization, methodology, formal analysis, supervision and writing J.W. and Y.C.; software, investigation, validation, and writing K.Y., Y.W., Z.L. and J.L. All authors have read and agreed to the published version of the manuscript.

Institutional Review Board Statement: Not applicable.

Data Availability Statement: The data presented in this study are available on request from the corresponding author.

Conflicts of Interest: The authors declare no conflict of interest.

References

1. Zhu, G.; Neises, T.; Turchi, C.; Bedilion, R. Thermodynamic evaluation of solar integration into a natural gas combined cycle power plant. *Renew. Energy* **2015**, *74*, 815–824. [CrossRef]
2. Wang, Y.; Bhattacharyya, D.; Turton, R. Evaluation of novel configurations of natural gas combined cycle (NGCC) power plants for load-following operation using dynamic modeling and optimization. *Energy Fuels* **2019**, *34*, 1053–1070. [CrossRef]
3. Impram, S.; Nese, S.V.; Oral, B. Challenges of renewable energy penetration on power system flexibility: A survey. *Energy Strategy Rev.* **2020**, *31*, 100539. [CrossRef]
4. Aliyu, M.; AlQudaihi, A.B.; Said, S.A.M.; Habib, M.A. Energy, exergy and parametric analysis of a combined cycle power plant. *Therm. Sci. Eng. Prog.* **2020**, *15*, 100450. [CrossRef]
5. Bahrami, S.; Ghaffari, A.; Genrup, M.; Thern, M. Performance comparison between steam injected gas turbine and combined cycle during frequency drops. *Energies* **2015**, *8*, 7582–7592. [CrossRef]
6. Smith, R.W. Steam turbine cycles and cycle design optimization: Combined cycle power plants. In *Advances in Steam Turbines for Modern Power Plants*; Woodhead Publishing: Sawston, UK, 2022; pp. 61–102.
7. Han, Y.; Feng, Y.; Yang, P.; Xu, L.; Zalhaf, A.S. An efficient algorithm for atomic decomposition of power quality disturbance signals using convolutional neural network. *Electr. Power Syst. Res.* **2022**, *206*, 107790. [CrossRef]
8. Tüfekci, P. Prediction of full load electrical power output of a base load operated combined cycle power plant using machine learning methods. *Int. J. Electr. Power Energy Syst.* **2014**, *60*, 126–140. [CrossRef]
9. Ghosh, T.; Martinsen, K.; Dan, P.K. Data-driven beetle antennae search algorithm for electrical power modeling of a combined cycle power plant. In Proceedings of the World Congress on Global Optimization, Metz, France, 8 July 2019.
10. Lorencin, I.; Anđelić, N.; Mrzljak, V.; Car, Z. Genetic algorithm approach to design of multi-layer perceptron for combined cycle power plant electrical power output estimation. *Energies* **2019**, *12*, 4352. [CrossRef]
11. Siddiqui, R.; Anwar, H.; Ullah, F.; Ullah, R.; Rehman, M.A.; Jan, N.; Zaman, F. Power Prediction of Combined Cycle Power Plant (CCPP) Using Machine Learning Algorithm-Based Paradigm. *Wirel. Commun. Mob. Comput.* **2021**, *2021*, 9966395. [CrossRef]
12. Therkorn, D. Remote monitoring and diagnostic for combined-cycle power plants. In Proceedings of the Turbo Expo: Power for Land, Sea, and Air, Reno, NV, USA, 6 June 2005; Volume 46997, pp. 697–703.
13. Davallo, H.E.; Bahrevar, R.; Chaibakhsh, A. Fault diagnosis of Combined Cycle Power Plant Using ELM. In Proceedings of the 2019 7th International Conference on Robotics and Mechatronics (ICRoM), Tehran, Iran, 20 November 2019; pp. 40–45.
14. Berrios, R.; Núñez, F.; Cipriano, A. Fault tolerant measurement system based on Takagi–Sugeno fuzzy models for a gas turbine in a combined cycle power plant. *Fuzzy Sets Syst.* **2011**, *174*, 114–130. [CrossRef]
15. Camporeale, S.; Dambrosio, L.; Milella, A.; Mastrovito, M.; Fortunato, B. Fault diagnosis of combined cycle gas turbine components using feed forward neural networks. In Proceedings of the Turbo Expo: Power for Land, Sea, and Air, Atlanta, GA, USA, 15–17 June 2003; Volume 36843, pp. 549–561.
16. Finn, J.; Wagner, J.; Bassily, H. Monitoring strategies for a combined cycle electric power generator. *Appl. Energy* **2010**, *87*, 2621–2627. [CrossRef]
17. Al-Tameemi, A.A.; Wang, K.; Li, L.; Zalhaf, A.S. A Convolutional Attention Mechanism-based Capsule Network scheme for Gearbox fault diagnosis using Two directions signals and Noise Environment. In Proceedings of the 2021 IEEE 5th Information Technology, Networking, Electronic and Automation Control Conference (ITNEC), Xi'an, China, 15 October 2021; Volume 5, pp. 91–100.
18. Yao, K.; Wang, Y.; Fan, S.; Wan, J.; Wu, H.; Cao, Y. Fault Mechanism and Diagnosis Method of Typical Load Mutation Problem of Turbo-generator Set. *Front. Energy Res.* **2020**, *10*, 1325. [CrossRef]
19. Qasem, M.A.; Albagul, A. Performance investigation of the gas turbine with the combined power plant. In Proceedings of the 2021 IEEE 1st International Maghreb Meeting of the Conference on Sciences and Techniques of Automatic Control and Computer Engineering MI-STA, Tripoli, Libya, 25 May 2021; pp. 485–490.
20. Yang, Q.; Li, S.; Cao, Y. A strong tracking filter based multiple model approach for gas turbine fault diagnosis. *J. Mech. Sci. Technol.* **2018**, *32*, 465–479. [CrossRef]
21. Yang, Q.; Li, S.; Cao, Y. Multiple model-based detection and estimation scheme for gas turbine sensor and gas path fault simultaneous diagnosis. *J. Mech. Sci. Technol.* **2019**, *33*, 1959–1972. [CrossRef]
22. Zhang, G.; Zheng, J.; Yang, Y.; Liu, W. Thermodynamic performance simulation and concise formulas for triple-pressure reheat HRSG of gas–steam combined cycle under off-design condition. *Energy Convers. Manag.* **2016**, *122*, 372–385. [CrossRef]
23. Kiaee, M.; Tousi, A.M. Vector-based deterioration index for gas turbine gas-path prognostics modeling framework. *Energy* **2021**, *216*, 119198. [CrossRef]